Picosecond Time-Resolved Fluorescence Studies Are Consistent with Reversible Excited-State Intramolecular Proton Transfer in 4′-(Dialkylamino)-3-hydroxyflavones

Vasyl V. Shynkar,[†,‡] Yves Mély,*[,†] Guy Duportail,[†] Etienne Piémont,[†] Andrey S. Klymchenko,[†,‡] and Alexander P. Demchenko[†,§,||]

Laboratoire de Pharmacologie et Physicochimie des interactions cellulaires et moléculaires, UMR 7034 du CNRS, Faculté de Pharmacie, Université Louis Pasteur, 67401 Illkirch, France, Departments of Physics and Chemistry, Kyiv National Taras Shevchenko University, 01033 Kyiv, Ukraine, TUBITAK Research Institute for Genetic Engineering and Biotechnology, Gebze-Kocaeli 41470, Turkey, and A. V. Palladin Institute of Biochemistry, 9 Leontovicha str., 01030 Kyiv, Ukraine

Received: June 29, 2003; In Final Form: September 10, 2003

Picosecond time-resolved fluorescence spectroscopy has been applied to the studies of excited-state intramolecular proton transfer (ESIPT) dynamics in two 4′-(dialkylamino)-3-hydroxyflavone derivatives (unsubstituted and substituted at the 6-position) in ethyl acetate and dichloromethane. In all the studied cases, the fluorescence decay kinetics of both short-wavelength normal (N*) and long-wavelength tautomer (T*) bands can be characterized by the same two lifetime components, which are constant over the all wavelength range of the emission. In the meantime, the preexponential factor of the short-lifetime component changes its sign, being positive for the N* and negative for the T* emission band. Moreover, the two preexponential factors of the T* emission decay are the same in magnitude but opposite in sign. These features are characteristic of a fast reversible two-state ESIPT reaction. Reconstruction of time-resolved spectra allows observing the evolution of these spectra with the appearance, rapid growth, and stabilization (in less than 200 ps) of the relative intensities of the two emission bands. A detailed kinetic model was applied for the analysis of these data, which involved the determination of radiative and nonradiative decay rate constants of both N* and T* forms and of forward and reverse rate constants for transitions between them. We show that ESIPT reaction in the studied conditions occurs on the scale of tens of picoseconds and thus is uncoupled with dielectric relaxations in the solvent occurring at subpicosecond times. Moreover, the radiative and nonradiative deactivation processes were found to be much slower than the ESIPT reaction, suggesting that the relative intensities of the two emission bands are mainly governed by the ESIPT equilibrium. Therefore, both electrochromic and solvatochromic effects on the relative intensities of the two emission bands in 4′-(dialkylamino)-3-hydroxyflavones result from the shifts in the ESIPT equilibrium.

Introduction

Excited-state intramolecular proton transfer (ESIPT) is the reaction that occurs between the proximate proton donor and acceptor groups connected by a H-bond on the same photoexcited molecule.[1−3] ESIPT is often considered as a prototype of proton-transfer reactions that are basic for chemistry and biochemistry. A variety of organic fluorophores exhibiting ESIPT has been described in the literature.[1−4] The classical example is 3-hydroxyflavone (3HF).[1,5] In contrast to ESIPT in systems with symmetric proton transfer (e.g., tropolone and 9-hydroxyphenalenone[2,3]), this reaction in 3HF occurs between structurally and energetically asymmetric states and generates in the excited state a species with changed electronic and nuclear configuration, the tautomer (T*) form. The latter is isomeric to the initially excited normal (N*) form and demonstrates a fluorescence spectrum dramatically shifted to lower energies (longer wavelengths), up to 5000−6000 cm^{-1}. In condensed media, the emission of the T* form can be easily observed in 3HF and its derivatives,[5−8] and the ground-state T form can be detected by transient spectroscopic techniques,[9] in line with the 4-level model originally suggested by Kasha[1,5] (Figure 1). In this model, the time-dependent evolution of the initially excited

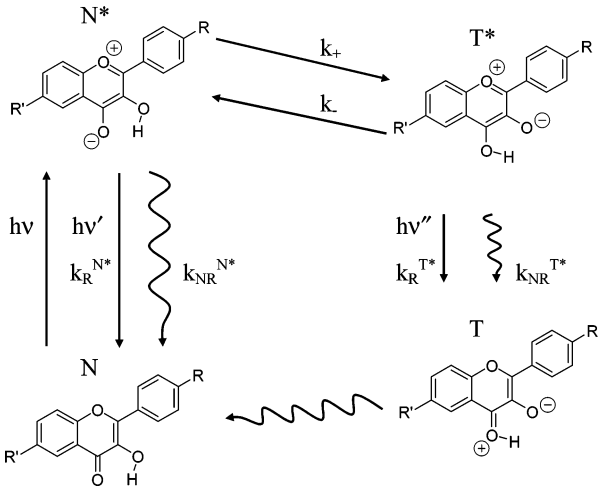

Figure 1. ESIPT reaction in 3-hydroxyflavone F and F2 derivatives. R = $N(CH_3)_2$ or $N(C_2H_5)_2$; R′ = H or $CH_2N^+(CH_3)_2C_8H_{17}(Br^-)$ for dyes F and F2, respectively.

* Corresponding author. Tel: +33 390 244263. Fax: +33 390 244313. E-mail: mely@aspirine.u-strasbg.fr.
† Université Louis Pasteur.
‡ Kyiv National Taras Shevchenko University.
§ TUBITAK Research Institute for Genetic Engineering and Biotechnology.
|| A. V. Palladin Institute of Biochemistry.

10.1021/jp035855n CCC: $25.00
Published on Web 10/18/2003

N* form should involve forward transition to the T* state (ESIPT) with a kinetic rate constant k_+ together with emissive and nonemissive conversion to the ground N state with kinetic constants $k_R^{N^*}$ and $k_{NR}^{N^*}$, respectively. Likewise, the decay of the T* state resulting from the ESIPT reaction can be characterized by reverse transition to the N* state with a rate constant k_- and by radiative (with rate constant $k_R^{T^*}$) and nonradiative (with rate constant $k_{NR}^{T^*}$) conversions to the ground T state. Therefore, according to this model, the kinetic description of photophysics of 3HF derivatives will include the determination of six kinetic rate constants. Interplay of these rate constants should form the contour of the steady-state spectrum with two characteristic bands.

ESIPT reaction for the parent 3HF in aprotic solvents is an extremely fast process occurring on the femtosecond time scale,[10,11] which explains the absence of the N* emission band in the steady-state spectra. This band becomes observable only in protic solvents, due to specific solvation of the N* form that breaks intramolecular hydrogen bond and thus uncouples ESIPT.[12−15] Surprisingly, the properties of 4′-dialkylamino-substituted 3HFs are quite different, because an intense N* emission band is observed in these derivatives in aprotic solvents such as acetonitrile and dichloromethane.[6,7,16] The presence of N* form in emission is not uncommon in ESIPT photochemistry, it can be observed for a number of other dyes. But in all these cases, this emission was explained by the existence of ground-state conformational isomers or a conformational isomerization in the N* state associated with a reorganization of the hydrogen bonds involved in proton transfer.[4,17−20] However, this explanation is not applicable for 3HF and its derivatives because the chromone ring is a rigid system that does not allow isomerization. One possible explanation for the observation of N* emission in dialkylamino-substituted 3HF derivatives is a solvent-reorganization barrier that retards the reaction. The origin of this barrier can be energetic and related to the interaction of the excited-state dipole μ_e with solvent dipoles. This barrier is thought to be high in dialkylamino-substituted derivatives because the introduction of the electron-donor dialkylamino group on the chromone ring is expected to provide a high μ_e value upon electronic excitation to the N* form.[21,22] This substitution may also produce a twisted intramolecular charge-transfer (TICT) state, which is stabilized stronger than the N* state.[8] In contrast, because the ESIPT reaction substantially decreases the dipole moment by compensating the separation of electronic charges existing in the N* state, the T* state should be much less subjected to solvent perturbations, and thus less dielectrically stabilized than the N* state. When the N* and T* states are of comparable energies, the ESIPT reaction may become reversible and an equilibrium can be established between these states. This may explain the increase of the relative intensity of the N* band with increased of polarity of aprotic solvents.[6,16] Selective electrostatic stabilization of the N* state with an introduced proximal charged group also results in a dramatic growth of its relative intensity,[23] which is also in line with the ESIPT equilibrium model. Linear dependence of the logarithm of the intensity ratio, I_{N^*}/I_{T^*}, on solvent polarity[16] and on the band separation[16] as well as the observation of a biexponential decay for the N emission band[6] are the arguments that support this model but still cannot be considered as direct evidence. Alternatively, it can be assumed that an intramolecular H-bond may become disrupted in these compounds even in aprotic solvents, and the dynamics of its rearrangement may limit the ESIPT rate.[8] From the examples of other ESIPT systems, it is known that when ESIPT occurs in solution, the reaction coordinate becomes multidimensional with the involvement of solvent coordinates.[20] This can result in complex reaction mechanisms, which may not exist in parent 3HF, but are present in 4′-(dialkylamino)-3HF.

As a consequence, important questions regarding the mechanism of ESIPT for the strongly solvatochromic 4′-(dialkylamino)-3HF derivatives remained unanswered. (1) Is this reaction intrinsically a two-state process or should it involve some intermediates, such as torsionally relaxed or solvent-stabilized N* forms, destabilized T* forms or solute−solvent excited-state complexes (exciplexes)? (2) Is this reaction intrinsically irreversible or reversible? (3) If it is reversible, then which mechanism is responsible for the solvatochromic and electrochromic variations of the relative intensities of the two bands in the steady-state spectrum? Are they a result of shifts in the ESIPT equilibrium or are they due to the slow forward ESIPT rate compared to the nonradiative deactivation rate?

To answer these questions, we performed a detailed picosecond time-resolved fluorescence study of two 3HF derivatives, F and F2 (Figure 1), that differ significantly by quantum yields and two-band emission properties, due to internal electrochromic effect in ionic F2.[23,24] Moreover, to analyze the possible solvatochromic modulation of ESIPT, the experiments were performed in two aprotic solvents of different polarity: ethyl acetate and dichloromethane.

Materials and Methods

4′-(Dimethylamino)-3-hydroxyflavone (F) and [4′-(diethylamino)-3-hydroxy-6-flavonyl](*N*,*N*,*N*-dimethyloctyl)ammonium bromide (F2) were synthesized as described elsewhere.[8,24] Ethyl acetate and dichloromethane were of spectroscopic grade.

Absorption and emission spectra were recorded on a Cary 400 spectrophotometer and a FluoroMax 3.0 (Jobin Yvon, Horiba) spectrofluorometer, respectively. Deconvolution of fluorescence spectra into two bands was performed using the program Siano, kindly provided by the author (A. O. Doroshenko from the Karazin University, Kharkov, Ukraine). The program uses an iterative nonlinear least-squares method based on the Fletcher−Powell algorithm. The shapes of the individual emission bands were approximated by a log-normal function,[25] which accounts for the asymmetry of the spectral bands. The fluorescence quantum yield (ϕ) was determined using solution of 4′-(diethylamino)-3-hydroxyflavone in ethanol as a reference ($\phi = 0.52$).[7]

Time-resolved fluorescence measurements were performed with the time-correlated, single-photon counting technique using the frequency doubled output of a Ti−Sapphire laser (Tsunami, Spectra Physics), pumped by a Millenia X laser (Tsunami, Spectra Physics).[26] The single-photon events were detected with a microchannel plate Hamamatsu R3809U photomultiplier coupled to a Philips 6954 pulse preamplifier and recorded on a multichannel analyzer (Ortec 7100) calibrated at 25.5 ps/channel. The instrumental response function was recorded with a polished aluminum reflector, and its full-width at half-maximum was 50 ps. The excitation wavelength was set at 430 nm. Time-resolved data were analyzed by the maximum entropy method using the Pulse 5.0 software.[27] Time-resolved emission spectra (TRES) were calculated by

$$I(\lambda,t) = \frac{F(\lambda)}{\sum \alpha_i(\lambda)\,\tau_i(\lambda)} \sum_{i=1}^{2} \alpha_i(\lambda)\,\exp[-t/\tau_i(\lambda)]$$

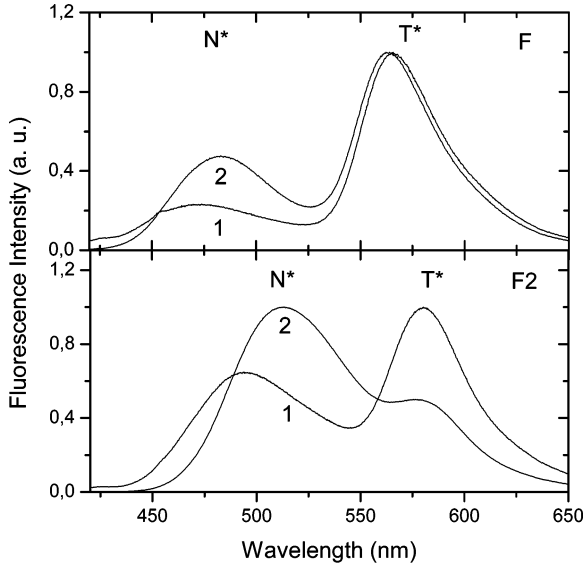

Figure 2. Steady-state fluorescence spectra of dyes F and F2 in ethyl acetate (1) and dichloromethane (2). Excitation wavelength was 430 nm.

where $F(\lambda)$ is the steady-state fluorescence intensity, $\tau_i(\lambda)$ are the decay times, and $\alpha_i(\lambda)$ are the relative amplitudes, with $\sum\alpha_i(\lambda) = 1$.[28]

Results

Steady-State Spectroscopy Data. The fluorescence properties of two 4′-dialkylamino-substituted flavones have been studied in two solvents of different polarity: ethyl acetate (dielectric constant $\epsilon = 6.02$) and dichloromethane ($\epsilon = 9.08$). We observe that in both solvents, the emission of the N* form is more pronounced for F2 than for F (Figure 2). This can be explained by an electrochromic modulation of ESIPT by the proximal positively charged ammonium group.[23] Regarding the solvatochromic effect, both F and F2 dyes show significantly higher relative intensity of the N* band in more polar dichloromethane as compared to ethyl acetate (Figure 2). Both the effects of proximal charge and of polarity result in a significant red shift of the N* band, which is much stronger than that of the T* band, in accordance with our previous data.[16,23] These results can be explained by a much higher dipole moment of the N* state in comparison to the T* state,[6,16,21] so that the electrochromic and solvatochromic effects can provide a selective stabilization of the former.

We also observe that the two solvents produce different quenching effects on F and F2 dyes. The fluorescence quantum yield of both dyes is lower in ethyl acetate (0.061 for F and 0.196 for F2) than in dichloromethane (0.151 for F and 0.685 for F2). This reflects a common regularity for 3HF derivatives: the lowest quantum yields are observed in hydrogen bond acceptor solvents, such as esters and ethers.[29]

To provide a definite answer, whether the ESIPT equilibrium model is able to describe the origin of the solvent-dependent two-band behavior of 4′-(dialkylamino)-3HFs, and how the excited-state deactivation processes affect this mechanism, we performed time-resolved fluorescence measurements over the whole emission spectrum.

Time-Resolved Emission Decays and Spectra. For an excited-state reaction between the N* and T* forms (Figure 1), the differential rate equations for the change of concentration of the N* and T* species, [N*] and [T*], with time are given by

$$\mathrm{d[N^*]}/\mathrm{d}t = -(k_R^{N^*} + k_{NR}^{N^*} + k_+)[N^*] + k_-[T^*] \quad (1)$$

$$\mathrm{d[T^*]}/\mathrm{d}t = -(k_R^{T^*} + k_{NR}^{T^*} + k_-)[T^*] + k_+[N^*] \quad (2)$$

The integration of eqs 1 and 2 with the initial boundary condition that only N* is directly excited and populated at time zero (i.e., at $t = 0$, $[N^*] = [N^*]_0$ and $[T^*] = 0$), yields the following equations for [N*] and [T*]:[30]

$$[N^*] = [N^*]_0(\alpha_1^{N^*}e^{-t/\tau_1} + \alpha_2^{N^*}e^{-t/\tau_2}) \quad (3)$$

$$[T^*] = [N^*]_0(\alpha_1^{T^*}e^{-t/\tau_1} + \alpha_2^{T^*}e^{-t/\tau_2}) \quad (4)$$

The decay times, τ_1 and τ_2, and preexponential amplitudes are related to the rate constants indicated in Figure 1 according to

$$\alpha_1^{N^*} = \frac{\gamma_{N^*} - \gamma_2}{\gamma_1 - \gamma_2} \quad (5)$$

$$\alpha_2^{N^*} = \frac{\gamma_1 - \gamma_{N^*}}{\gamma_1 - \gamma_2} \quad (6)$$

$$-\alpha_1^{T^*} = \alpha_2^{T^*} \quad (7)$$

where

$$\gamma_1,\gamma_2 = \tau_1^{-1},\tau_2^{-1} = {}^1/_2\{(\gamma_{N^*} + \gamma_{T^*}) \pm [(\gamma_{N^*} - \gamma_{T^*})^2 + 4k_-k_+]^{1/2}\} \quad (8)$$

with $\gamma_{N^*} = k_R^{N^*} + k_{NR}^{N^*} + k_+$ and $\gamma_{T^*} = k_R^{T^*} + k_{NR}^{T^*} + k_-$.

When the ESIPT reaction between N* and T* states is reversible, then as shown by eqs 3−7 the two decay times of the N* and T* forms should be characterized by the same τ_1 and τ_2 values. Moreover, the two preexponential factors describing the growth and decay of [T*] should be identical in magnitude but opposite in sign.[31,32] These features can be used as relevant criteria for the application of the reversible model described in Figure 1.

To check if the reversible model applies to excited-state dynamics of F and F2, we monitored their time-resolved intensity decays in ethyl acetate and dichloromethane. As a representative example, Figure 3 shows the time-resolved intensity decay of dye F2 in ethyl acetate recorded at emission wavelengths of 490 nm (A) and 600 nm (B). At these wavelengths the decays of N* and T* forms, respectively, can be selectively monitored. To provide a model-independent deconvolution of decays, the maximum entropy method[27] was used. The decay of the N* form was found to follow a biexponential function with a shorter component of 51 ps associated with a 67 % amplitude and a longer component of 700 ps (Table 1). No improvement of the fit was obtained for this form if negative amplitudes were allowed in MEM analysis (data not shown). In contrast, when negative amplitudes were allowed for the analysis of the T* form decay, a dramatic improvement of the fit was obtained (compare traces 3 and 4 in Figure 3B). The presence of a component with negative amplitude is already obvious from the decay curve itself (trace 1 in Figure 3B) showing a rise in the initial channels, which is characteristic for excited-state reactions.[28,30] Importantly, the lifetimes of the N* and T* forms were found to be the same. Moreover, the two pre-exponential factors associated with T*

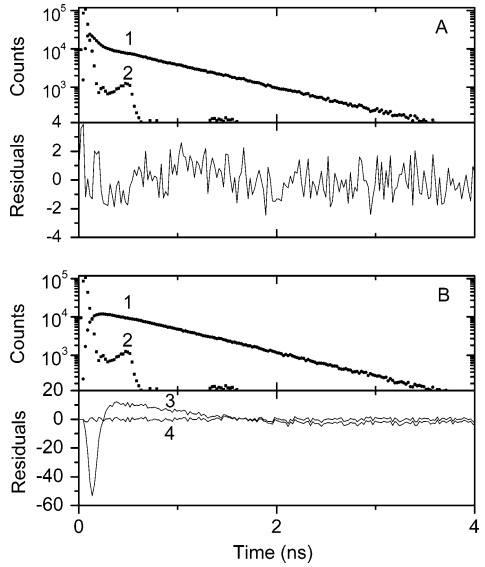

Figure 3. Intensity decay profile of probe F2 in ethyl acetate. Excitation wavelength was 430 nm. (1) Emission decay; (2) instrument response function. (A) Emission of N* form observed at 490 nm. Residuals correspond to a two-component analysis with the positive preexponential factors given in Table 1. (B) Emission of T* form observed at 600 nm. Residuals correspond to a two-component analysis with either two positive preexponential factors (3) or both positive and negative preexponential factors (4).

TABLE 1: Time-Resolved Fluorescence Parameters at the Two Emission Bands and Quantum Yields of F and F2 Dyes in Ethyl Acetate and Dichloromethane[a]

dye	solvent	band	τ_1, ns	α_1[b]	τ_2, ns	α_2[b]	Q
F	ethyl acetate	N*	0.038	0.87	0.31	0.13	0.014
		T*	0.038	−0.49	0.33	0.51	0.047
	dichloromethane	N*	0.061	0.78	0.65	0.22	0.049
		T*	0.053	−0.47	0.65	0.53	0.102
F2	ethyl acetate	N*	0.051	0.67	0.70	0.33	0.092
		T*	0.055	−0.44	0.64	0.56	0.104
	dichloromethane	N*	0.082	0.24	2.16	0.76	0.586
		T*	0.071	−0.50	2.05	0.50	0.099

[a] τ_1 and τ_2 are fluorescence lifetimes; α_1 and α_2 are preexponential coefficients. The excitation wavelength was 430 nm. The time-resolved data for the N* and T* bands were recorded at 490 and 600 nm, respectively. [b] α_1 and α_2 values were normalized according to $|\alpha_1| + |\alpha_2| = 1$.

emission decay ($\alpha_1^{T^*}$ and $\alpha_2^{T^*}$) are of similar amplitude and opposite in sign. These data are in excellent agreement with a model of reversible ESIPT reaction[31] that proceeds in the 10−100 ps time range. This conclusion is also in line with the data previously reported on dye F in benzene/acetonitrile solvent mixtures.[6] The same behavior is observed for both F and F2 in the two studied solvents (Table 1). This suggests that the reversibility of the fast ESIPT reaction is a general feature for 4′-dialkylamino-substituted 3HF derivatives.

Both F and F2 dyes exhibit much higher lifetime values in dichloromethane than in ethyl acetate, in line with the trends observed for the quantum yields (Table 1). Moreover, in line with the higher quantum yield of F2 with respect to F in both solvents, both the short and long lifetimes of F2 are higher than the corresponding lifetimes of F. Importantly, the increase of solvent polarity from ethyl acetate to dichloromethane decreases significantly the ratio of amplitudes, α_1/α_2, associated with the N* band lifetimes. A substantial decrease of the α_1/α_2 ratio also results from introduction in F2 of the cationic group.

To further validate the relevance of the reversible reaction model, the fluorescence intensity decays of both F and F2 dyes

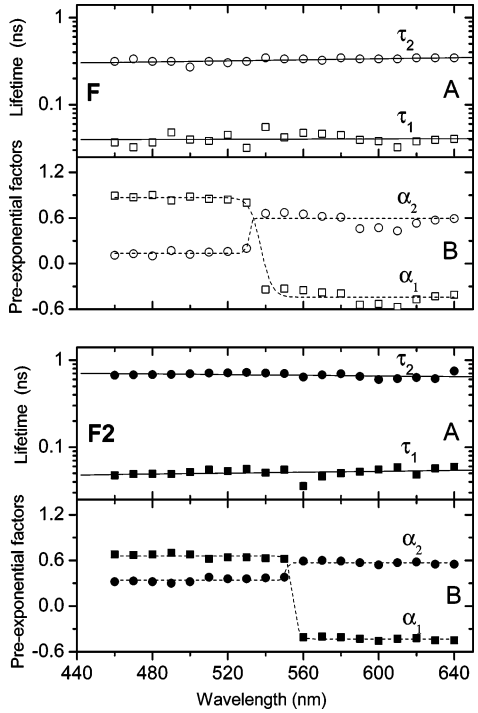

Figure 4. Emission wavelength dependence of the time-resolved parameters of dyes F (open symbols) and F2 (filled symbols) in ethyl acetate. Excitation wavelength was 430 nm. The time-resolved parameters were obtained using MEM method. (A) Lifetimes of the short-lived (τ_1) and long-lived (τ_2) components. (B) Associated preexponential factors, α_1 and α_2.

in ethyl acetate were studied as a function of emission wavelength (Figure 4). Both short- and long-lived lifetimes of the two dyes were found constant over the investigated spectral range (Figure 4A). In contrast, a clear discontinuity is observed for both preexponential factors (Figure 4B) at the wavelengths, where the N* and T* bands overlap (530−540 nm for F and 550−560 nm for F2). At these wavelengths, the amplitudes of the short-lived components change in sign from positive to negative and their absolute values become equal to that of the long-lived components.

The data on the emission wavelength dependence of decay kinetics were used to calculate the time-resolved emission spectra (TRES) of both F and F2 dyes in ethyl acetate.[33] These spectra allow us to observe the redistribution with time of emissive species between the N* and T* bands (Figure 5). Already at 10 ps, we observe together with the major N* emission component, a significant emission from the T* state. The relative amount of the latter increases with time and reaches a maximum at about 100 ps. After 100 ps, the spectra do not change their two-band shape significantly, and a simultaneous decrease of intensity is observed for both bands. These results provide an additional demonstration that ESIPT reaction proceeds in the 10−100 ps time range and is faster than other deactivation processes.

To describe how the ESIPT equilibrium is established with time, we analyzed the time-dependence of the relative populations of the two states, [T*]/[N*]. The latter were obtained from eq 3 and 4, using the experimental lifetimes and preexponential coefficients.[33] As seen from Figure 6, [T*]/[N*] increases nonlinearly with time and reaches an equilibrium value after ca. 200 ps. It appears clearly that the time required for the populations of the two states to reach the equilibrium value is much shorter than the long-lived lifetime values in all cases, except for F in ethyl acetate.

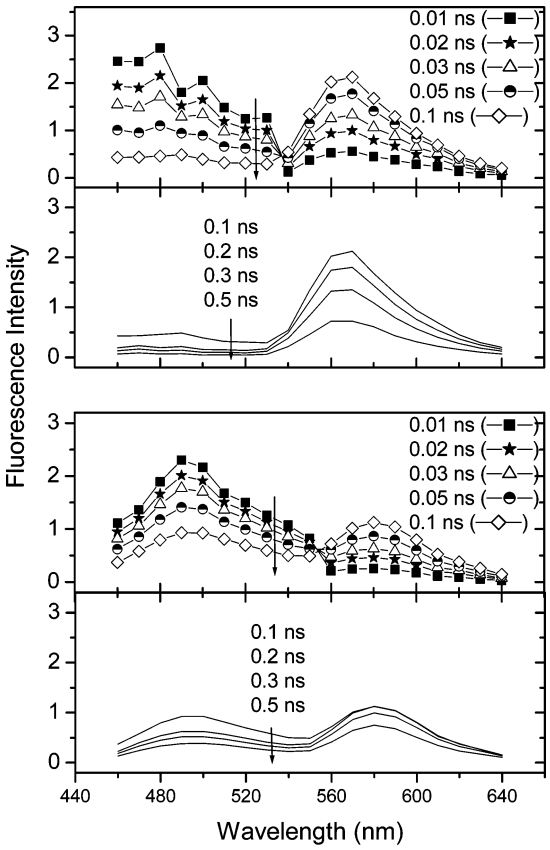

Figure 5. Time-resolved emission spectra for dyes F (above) and F2 (below) in ethyl acetate.

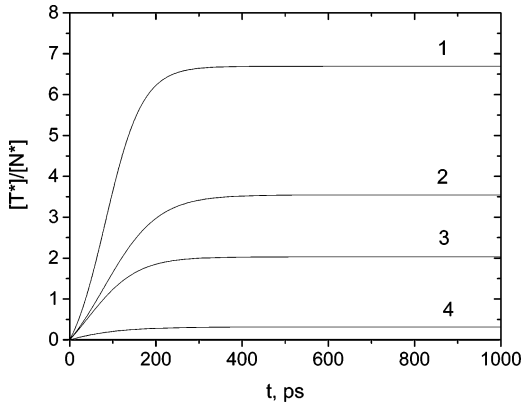

Figure 6. Relative populations of the N* and T* excited states for F and F2 dyes as a function of time: (1) F in ethyl acetate; (2) F in dichloromethane; (3) F2 in ethyl acetate; (4) F2 in dichloromethane.

On a next step, the γ_{N^*} and γ_{T^*} values were calculated from eqs 5−8 by

$$\gamma_{N^*} = \gamma_2 + \alpha_1^{N^*}(\gamma_1 - \gamma_2) \tag{9}$$

$$\gamma_{T^*} = \gamma_1 - \alpha_1^{N^*}(\gamma_1 - \gamma_2) \tag{10}$$

and presented in Table 2. To independently assess the relevance of the calculated γ_{T^*} values, the differential method[34] was used. This method relies on the fact that the population of the T* state can be considered as a convolution integral with the N* state. In this respect, deconvolving the T* state emission with the N* state emission (considered thus as a response function) yields the lifetime ($\tau_{T^*}^{exp} = (\gamma_{T^*}^{exp})^{-1}$) of the T* state that would be observed if the T* state could be directly excited. The application of this procedure requires a spectral region where the emission from the N* state could be observed without overlap from that of the T* state. This is assumed to be achieved in the blue edge of the N* band. For both F and F2 compounds, $\gamma_{T^*}^{exp}$, the inverse of the $\tau_{T^*}^{exp}$ lifetime directly measured by this differential method is in excellent agreement with the γ_{T^*} value calculated from eq 10 (Table 2).

TABLE 2: Kinetic Constants Calculated on the Basis of Fluorescence Decay Data and Quantum Yields

	F		F2	
solvent	EtOAc	CH_2Cl_2	EtOAc	CH_2Cl_2
$10^{-9}\gamma_{N^*}$ (s^{-1})	22.0	13.2	13.3	3.5
$10^{-9}\gamma_{T^*}$ (s^{-1})	6.2	4.9	7.6	8.5
$10^{-9}\gamma_{T^*}^{exp}$ (s^{-1})	5.7	4.7	6.9	8.5
$10^{-9}(\gamma_{N^*}+\gamma_{T^*})$ (s^{-1})	28.1	18.2	20.8	11.9
$10^{-9}\gamma_1$ (s^{-1})	26.3	16.4	19.6	12.2
K_γ	3.6	2.7	1.75	0.41
K_α	6.7	3.5	2.0	0.32
Q_{T^*}/Q_{N^*}	3.4	2.1	1.13	0.17
$10^{-9}k_R^{N^*}$ (s^{-1})	0.19	0.26	0.35	0.36
$k_R^{T^*}/k_R^{N^*}$	0.50	0.59	0.56	0.53
$10^{-9}k_R^{T^*}$ (s^{-1})	0.10	0.15	0.20	0.19
$10^{-9}k_R$ (s^{-1})	0.20 (0.11)	0.23 (0.18)	0.28 (0.25)	0.32 (0.32)
$10^{-9}k_{NR}$ (s^{-1})	3.0	1.31	1.15	0.15

[a] γ_{N^*} and γ_{T^*} are the decay rate constants of N* and T* bands, respectively. $\gamma_{T^*}^{exp}$ was measured by the differential method, as described in the text. If ESIPT rate constants are much higher than radiative and nonradiative rate constants then γ_{N^*} and γ_{T^*} correspond to the forward and reverse rate constants, k_+ and k_-, respectively. K_γ ($=\gamma_{N^*}/\gamma_{T^*}$) and K_α ($=\alpha_1/\alpha_2$) describe the equilibrium constant of the ESIPT. Q_{N^*} and Q_{T^*} correspond to the quantum yields of the N* and T* bands, respectively. The radiative rate constants of N* and T* forms, $k_R^{N^*}$ and $k_R^{T^*}$, were calculated as described in the text. The overall radiative rate constant, k_R, was calculated from the right and left (numbers in brackets) parts of eq 21.

Moreover, on the basis of the present data and those reported earlier for F in acetonitrile/benzene mixtures,[6] we may assume that the ESIPT reaction is much faster than the radiative and nonradiative deactivation processes, so that $k_+, k_- \gg k_R + k_{NR}$. Then eq 8 can be simplified:[35,36]

$$\gamma_{N^*} \cong k_+ \quad \text{and} \quad \gamma_{T^*} \cong k_- \tag{11}$$

$$\gamma_1 = k_+ + k_- \tag{12}$$

$$\gamma_2 = (k_R^{T^*} + k_{NR}^{T^*})\left(\frac{k_+}{k_+ + k_-}\right) + (k_R^{N^*} + k_{NR}^{N^*})\left(\frac{k_-}{k_+ + k_-}\right) \tag{13}$$

It follows that the measured short-lived component describes the ESIPT kinetics, whereas the long-lived component describes the radiative and nonradiative deactivation processes weighted by the partition of N* and T* forms in the excited state. Importantly, the experimental γ_1 values ($=\tau_1^{-1}$) are very similar to the $k_+ + k_-$ values expressed as $\gamma_{N^*} + \gamma_{T^*}$ (Table 2) in all four studied cases, suggesting that the ESIPT reaction is indeed much faster that the deactivation processes, so that most part of the emission proceeds after the species populating N* and T* states reach dynamic equilibrium.

Taken together, our data allow us to apply a simplified model for the calculation of the kinetic parameters, based on the consideration of ESIPT resulting in rapid two-state equilibrium.

ESIPT Dynamics. On the basis of eq 11, we may define the equilibrium constant K and express it as

$$K = k_+/k_- \cong \gamma_{N^*}/\gamma_{T^*} (=K_\gamma) \tag{14}$$

An alternative possibility to estimate the equilibrium constant is provided by a simplified solution of eqs 3−4:[6]

$$K = k_+/k_- \cong [\mathrm{T}^*]/[\mathrm{N}^*]\ (t \rightarrow \infty) = \alpha_1^{\mathrm{N}^*}/\alpha_2^{\mathrm{N}^*}\ (=K_\alpha) \qquad (15)$$

Both approximations (eqs 14 and 15) are based on the assumption that ESIPT reaction is much faster than the deactivation processes. Noticeably, this approximation is less applicable in eq 14 than in eq 15 when $K \gg 1$ or $K \ll 1$, because in these cases k_- or k_+ values, respectively, become small and comparable in magnitude with the corresponding deactivation constants (so that $\gamma_{\mathrm{T}^*} > k_-$ or $\gamma_{\mathrm{N}^*} > k_+$, respectively).

The calculated values of γ_{N^*}, γ_{T^*}, K_γ, and K_α are given in Table 2. It can be seen that the K_γ and K_α values match closely, except for F in ethyl acetate. As described above, this latter discrepancy is probably because $\gamma_{\mathrm{T}^*} > k_-$, so that the K_γ value appears abnormally low. The parameter K is an important characteristic of the ESIPT reaction and depends strongly on solvent polarity and the presence of a cationic group in F2. Indeed, for both F and F2 dyes, an increase in solvent polarity results in a significant decrease of K, and thus, a shift in ESIPT equilibrium toward the N* state. This is in accordance with the previously reported kinetic data of F in toluene/acetonitrile solvent mixtures[6] and the detailed steady-state solvatochromic data of a diethylamino analogue of F.[16] Decreased K values for flavone F2 as compared to F indicate that the introduction of a cationic group producing an electrochromic effect also shifts the ESIPT equilibrium toward the N* state, in line with previous steady-state data.[23] Importantly, both solvatochromic and electrochromic effects on K values correlate well with the changes of the quantum yield ratio between the two emission bands $Q_{\mathrm{T}^*}/Q_{\mathrm{N}^*}$ (Table 2). This fact demonstrates that in all studied cases we used reasonable approximations, so that the changes of nonradiative rate constants do not contribute significantly to variations of the relative intensities of the two bands. The only partial exception is F in ethyl acetate, where the fluorescence quantum yield is low and the difference between rates of ESIPT and deactivation processes are probably smaller.

Determination of Radiative and Nonradiative Rate Constants. Using the time-resolved decay parameters and the quantum yield of the N* band, the radiative rate constant for the N* state may be calculated by

$$k_{\mathrm{R}}^{\mathrm{N}^*} = Q_{\mathrm{N}^*}/(\alpha_1^{\mathrm{N}^*}\tau_1 + \alpha_2^{\mathrm{N}^*}\tau_2) \qquad (16)$$

Then, on the basis of the approximation of fast ESIPT equilibrium, we can write

$$\frac{Q_{\mathrm{T}^*}}{Q_{\mathrm{N}^*}} = \frac{k_{\mathrm{R}}^{\mathrm{T}^*}[\mathrm{T}^*]}{k_{\mathrm{R}}^{\mathrm{N}^*}[\mathrm{N}^*]} \qquad (17)$$

Because $K = [\mathrm{T}^*]/[\mathrm{N}^*]$, the ratio of rate constants can thus be expressed as

$$\frac{k_{\mathrm{R}}^{\mathrm{T}^*}}{k_{\mathrm{R}}^{\mathrm{N}^*}} = \frac{Q_{\mathrm{T}^*}}{KQ_{\mathrm{N}^*}} \qquad (18)$$

Importantly, the ratios of rate constants were found to be similar for all the studied cases (Table 2), suggesting that the relative oscillator strengths of the N*−N and T*−T transitions do not change significantly with the provided perturbations. Moreover, the $k_{\mathrm{R}}^{\mathrm{T}^*}$ values obtained from eq 18 were found to be about 2 times lower than the $k_{\mathrm{R}}^{\mathrm{N}^*}$ values in all the cases, demonstrating that the oscillator strength of the T*−T transition is probably 2 times smaller than the oscillator strength of the N*−N transition.

On the basis of the approximation that the ESIPT reaction is much faster than the deactivation processes, the overall quantum yield Q can be simply expressed as

$$Q = \frac{k_{\mathrm{R}}^{\mathrm{N}^*} + Kk_{\mathrm{R}}^{\mathrm{T}^*}}{k_{\mathrm{R}}^{\mathrm{N}^*} + Kk_{\mathrm{R}}^{\mathrm{T}^*} + k_{\mathrm{NR}}^{\mathrm{N}^*} + Kk_{\mathrm{NR}}^{\mathrm{T}^*}} \qquad (19)$$

Moreover, eq 13 can be rewritten as

$$1/\tau_2 = (k_{\mathrm{R}}^{\mathrm{T}^*} + k_{\mathrm{NR}}^{\mathrm{T}^*})\left(\frac{K}{K+1}\right) + (k_{\mathrm{R}}^{\mathrm{N}^*} + k_{\mathrm{NR}}^{\mathrm{N}^*})\left(\frac{1}{K+1}\right) \qquad (20)$$

and combined with eq 19 to yield

$$k_{\mathrm{R}}^{\mathrm{N}^*} + Kk_{\mathrm{R}}^{\mathrm{T}^*}/(1+K) = Q/\tau_2 = k_{\mathrm{R}} \qquad (21)$$

and

$$k_{\mathrm{NR}}^{\mathrm{N}^*} + Kk_{\mathrm{NR}}^{\mathrm{T}^*}/(1+K) = (1-Q)/\tau_2 = k_{\mathrm{NR}} \qquad (22)$$

where k_{R} and k_{NR} describe respectively the overall radiative and nonradiative rate constants of the excited molecule in the ESIPT equilibrium. It follows that the k_{R} values may be calculated either directly from overall quantum yield and lifetime τ_2 (right part of eq 21) or from the kinetic constants (left part of eq 21). The close similarity of the values obtained by these two approaches (Table 2) provides additional evidence for the proposed two-state equilibrium model. It allows describing ESIPT dynamics and calculating the kinetic parameters of the system with a good approximation. However, this model appears less valid for dyes with low Q values and short τ_2 lifetimes. Indeed, in contrast to the three other cases, the rates of nonradiative deactivation of F in ethyl acetate are comparable with ESIPT rate constants and, thus, could not be neglected.

Discussion

Model of Reversible Two-State Reaction. For parent 3HF, the ESIPT reaction kinetics in free jets and matrix-isolated systems is observed in the femtosecond time range.[10,11] It is thought to occur without activation barrier through proton-tunneling along the reaction coordinate connecting proximate proton-donor and proton-acceptor groups and thus is very fast. This reaction is also very fast in solutions, and according to some authors, it could be analogous to solvent-activated adiabatic electron transfer.[37,38] A different picture is observed for 4′-dialkylamino-substituted derivatives, for which the ESIPT reaction is strongly retarded,[6] especially in polar solvents. In (dialkylamino)-3HFs, the N* state is essentially a charge-transfer (CT) state.[21,22,39] Thus, after initial excitation to the Franck−Condon state, a rapid transition to CT state should occur, being followed by solvent relaxation. This raises the question on the coupling between solvent relaxation and ESIPT reaction. Several arguments strongly suggest that solvent reorganization dynamics (and other relaxation processes, like torsional motions) are not coupled directly with ESIPT. First, the ESIPT rate constants observed in this study are about 1−2 orders of magnitude slower than the dielectric relaxation rates in common aprotic low-viscous organic solvents.[40] Second, there are no indications of inhomogeneous kinetics that are characteristic for slowly relaxing systems.[41,42] Indeed, the intensity ratio, $I_{\mathrm{N}^*}/I_{\mathrm{T}^*}$, in the steady-state spectra does not depend on the excitation wave-

length (data not shown), and in time-resolved experiments, the shorter lifetime τ_1 does not change over the N* emission band (Figure 4).

Accordingly, because solvent relaxation occurs on a much faster time scale, the N* and T* states can be considered as dielectrically stabilized. The ESIPT reaction occurs in the conditions of solvation equilibrium, the solvent-unrelaxed states are not involved, and the relative intensity of the two emission bands of both F and F2 dyes are controlled predominantly by the ESIPT equilibrium. To provide direct experimental evidence for the reversibility of ESIPT reaction and determine the radiative and nonradiative rate constants for both excited states, the intensity decays of F and F2 were recorded with picosecond resolution at different wavelengths over all the emission spectrum. In full agreement with a reversible two-state process,[31] (a) a short lifetime τ_1 with a positive preexponential coefficient is observed for the N* band, whereas for the T* band, the same lifetime is associated with a negative preexponential component, (b) the long lifetimes associated with N* and T* bands are the same over the whole spectrum, and (c) the preexponential coefficients for the T* band emission decay are opposite in sign and of the same magnitude.

Our data underline the important differences between the parent 3HF and its 4′-dialkylamino-substituted derivatives. In parent 3HF, slow ESIPT kinetics (in the picosecond time range) occurs only in protic solvents where the solvent hydrogen bonding with the dye may produce an activation barrier.[13−15] In this case, the reaction being irreversible is characterized by the fact that the long-lived component of the T* state is remarkably longer than the corresponding component of the N* state.[13−15] This feature has never been observed in our case, suggesting that whereas in the parent 3HF the ESIPT reaction is kinetically controlled, for its 4′-dialkylamino derivatives it is under thermodynamic control, i.e., determined by the relative energies of the N* and T* states.

ESIPT Reaction Provides a Fast Equilibrium between the N* and T* States. According to our data, the ESIPT reaction appears to be much faster than radiative and nonradiative excited-state deactivations. This feature was notably deduced from the fact that the short-lived lifetime component (τ_1) in all four cases is 1 order of magnitude smaller than the corresponding long-lived component (τ_2), in line with the previously reported data on flavone F in acetonitrile/benzene mixtures.[6] Moreover, our data further suggest that the ESIPT equilibrium is reached on the early step of emission (within 100−200 ps). After this time, the shapes of emission spectra do not further change with time and are close to the corresponding steady-state spectra.

Because ESIPT reaction is reversible and occurs much faster than the emission decay, it follows that the observed strong solvatochromic and electrochromic effects in the electron-donor-substituted 3HFs are due to shifts in the ESIPT equilibrium. The N* state possesses a significantly higher dipole moment as compared to that of T* state, resulting in much stronger solvatochromic response.[16] Indeed, the N* band shows strong positive solvatochromy, whereas the T* band is almost independent of the solvent polarity. It follows that an increase of solvent polarity results in a stronger dielectric stabilization of the N* state as compared to the T* state, leading to a shift of ESIPT equilibrium toward the N* state. Likewise, the introduction of a cationic group in the case of F2 provides a strong Stark effect that stabilizes selectively the N* state and dramatically shifts the ESIPT equilibrium toward this state.[23] Moreover, the similarity between the K values calculated from the time-resolved data and those calculated from the ratios of quantum yields of the two forms, further suggests that the dual emission is controlled by the Boltzmann distribution of the relative populations of the N* and T* states at equilibrium.

Radiative and Nonradiative Rate Constants. Our data indicate that the radiative rate constants of N* and T* states, $k_R^{N^*}$ and $k_R^{T^*}$, for both F and F2 dyes are almost independent of solvent. This suggests that the mechanism of emission remains unchanged, and the formation of specific solute−solvent complexes can be excluded. Furthermore, the absolute values of these constants are almost 2 orders of magnitude smaller than the ESIPT rate constants, excluding a direct influence of the radiative processes on establishment of ESIPT equilibrium. It is important to note that the radiative rate constants for the N* emission are about twice as high as those of the T* emission, suggesting a higher oscillator strength of the N−N* transition,[43] due to the stronger charge-transfer character of the N* state compared to that of the T* state.

In contrast to the radiative rate constants, the nonradiative rate constants depend significantly on the solvent. Indeed, the nonradiative rate constants of F and F2 were found to be much larger in ethyl acetate than in dichloromethane (Table 2). Because the decrease in the quantum yield of 3HF derivatives in hydrogen-bond acceptor solvents was previously shown to be related to the formation of hydrogen bonds of the 3-OH group with the solvent molecules,[29] it may be suggested that this H-bond formation is also responsible for the increase in the k_{NR} value. Moreover, from the comparison of F and F2, it may be further concluded that electrostatic stabilization of the N* state with the cationic group significantly decreases the nonradiative rate constant.

Importantly, the k_{NR} values are substantially lower than the ESIPT rate constants for all the cases (except F in ethyl acetate), suggesting that nonradiative processes should not play a significant role in the establishment of the two-band profile of the steady-state spectrum. The absence of correlation between the fluorescence quantum yields and the intensity ratios of the emission bands further support this conclusion. The independence of these two parameters was already shown by extensive steady-state solvatochromic studies on an F analogue 4′-(diethylamino)-3-hydroxyflavone (FE).[16] If these parameters are coupled, then the decrease of nonradiative decay rate (increase of the quantum yield) should result in an increase of the T* emission intensity (because in this case longer times are allowed for the forward ESIPT to proceed). Because an exactly opposite result was observed, it may be concluded that the establishment of ESIPT equilibrium does not depend on the radiative or nonradiative deactivations of the excited state.

Our results also demonstrate that the model based on fast ESIPT equilibrium is limited when the quantum yield of the dye is low. In this case, the nonradiative deactivation rate becomes comparable with the ESIPT rate and the equilibrium constants calculated from the ratios of T* to N* quantum yields deviate from the equilibrium constants, K_α or K_γ, calculated from the lifetime measurements. This is particularly observed for F in ethyl acetate, where the quantum yield ratio is significantly lower than the K_α or K_γ values. However, the model works well for 3HF dyes that have quantum yields higher than 0.1 and allows us to confidently determine the rate constants. In all these cases, the dramatic changes in the dual emission of 4′-(dialkylamino)-3HFs are a result of the shifts in ESIPT equilibrium due to solvatochromic and electrochromic effects.

The results of the present study provide us the strategy for the development of new two-band ratiometric probes based on

3HF derivatives.[24,44,45] It should be based on the fact that unless the fluorescence quantum yield is very low, the relative intensities of N* and T* bands are guided by the conditions of the ESIPT equilibrium. Because the latter can be controlled in a predictable way by chemical substituents[46] and the properties of probe environment,[16] it becomes possible to design new fluorescence dyes with programmed two-band fluorescence and sensing properties.

Acknowledgment. This work was supported by grants from the CNRS, Université Louis Pasteur and TUBITAK. V.S. is a student of the European Doctoral College. A.D. and A.K. are fellows from the Université Louis Pasteur and the CNRS, respectively. We are grateful to A. O. Doroshenko, V. G. Pivovarenko, E. A. Posokhov, and M. Maroncelli for useful comments.

References and Notes

(1) Kasha, M. *J. Chem. Soc., Faraday Trans. 2* **1986**, *82*, 2379−2392.
(2) Barbara, P. F.; Walsh, P. K.; Brus, L. E. *J. Phys. Chem.* **1989**, *93*, 29−34.
(3) Formosinho, S. J.; Arnaut, L. G. *J. Photochem. Photobiol. A: Chem.* **1993**, *75*, 21−48.
(4) Douhal, A.; Lahmani, F.; Zewail, A. H. *Chem. Phys.* **1996**, *207*, 477−498.
(5) Sengupta, P. K.; Kasha, M. *Chem. Phys. Lett.* **1979**, *68*, 382−385.
(6) Swiney, T. C.; Kelley, F. D. *J. Chem. Phys.* **1993**, *99*, 211−221.
(7) Chou, P. T.; Martinez, M. L.; Clements, J. H. *J. Phys. Chem.* **1993**, *97*, 2618−2622.
(8) Ormson, M. S.; Brown, R. G.; Vollmer, F.; Rettig, W. *J. Photochem. Photobiol*. **1994**, *81*, 65−72.
(9) Itoh, M.; Yuzawa, T.; Mukaihata, H.; Hamaguchi, H. *Chem. Phys. Lett.* **1995**, *233*, 550−554.
(10) (a) Schwarz, B. J.; Peteanu, L. A.; Harris, C. B. J. *J. Phys. Chem.* **1992**, *96*, 3591−3598. (b) Ameer-Beg, S.; Ormson, S. M.; Brown, R. G.; Matousek, P.; Towrie, M.; Nibbering, E. T. J.; Foggi, P.; Neuwahl, F. V. R. *J. Phys. Chem. A* **2001**, *105*, 3709−3718.
(11) Bader, A. N.; Ariese, F.; Gooijer, C. *J. Phys. Chem. A* **2002**, *106*, 2844−2849.
(12) McMorrow, D.; Kasha, M. *J. Phys. Chem.* **1984**, *88*, 2235−2243
(13) Strandjord, A. J. G.; Barbara, P. F. *Chem. Phys. Lett.* **1983**, *98*, 21−26.
(14) Strandjord, A. J. G.; Courtney, S. H.; Friedrich, D. M.; Barbara, P. F. *J. Phys. Chem.* **1983**, *87*, 1125−1133.
(15) Strandjord, A. J. G.; Barbara, P. F. *J. Phys. Chem.* **1985**, *89*, 2355−2361.
(16) Klymchenko, A. S.; Demchenko, A. P. *Phys. Chem. Chem. Phys.* **2003**, *5*, 461−468.
(17) Henary, M. M.; Fahrni, C. J. *J. Phys. Chem. A* **2002**, *106*, 2510−2520.
(18) Mateo, C. R.; Douhal, A. *Proc. Natl. Acad. Sci. U.S.A.* **1998**, *95*, 7245−7250.
(19) (a) Santra, S.; Krishnamoorthy, G.; Dogra, S. K. *Chem. Phys. Lett.* **1999**, *311*, 55−61. (b) LeGourrierec, D.; Kharlanov, V. A.; Brown, R. G.; Rettig, W. *J. Photochem. Photobiol. A: Chem.* **2000**, *130*, 101−111.
(20) Waluk, J. In *Conformational analysis of Molecules in Excited States*; Waluk, J., Ed.; Wiley-VCH: New York, 2000; Chapter 2.
(21) Nemkovich, N. A.; Kruchenok, J. V.; Rubinov, A. N.; Pivovarenko, V. G.; Baumann, W. *J. Photochem. Photobiol. A: Chem.* **2001**, *139*, 53−62.
(22) Nemkovich, N. A.; Baumann, W.; Pivovarenko, V. G. *J. Photochem. Photobiol. A* **2002**, *153*, 19−24.
(23) Klymchenko, A. S.; Demchenko, A. P. *J. Am. Chem. Soc.* **2002**, *124*, 12372−12379.
(24) Klymchenko, A. S.; Duportail, G.; Ozturk, T.; Pivovarenko, V. G.; Mély, Y.; Demchenko, A. P. *Chem. Biol.* **2002**, *9*, 1199−1208.
(25) Siano, D. B.; Metzler, D. E. *J. Chem. Phys.* **1969**, *51*, 1856−1861.
(26) Bernacchi, S.; Stoylov, S.; Piémont, E.; Ficheux, D.; Roques, B. P.; Darlix, J. L.; Mély, Y. *J. Mol. Biol.* **2002**, *317*, 385−399.
(27) (a) Livesey, A. K.; Brochon. J.-C. *Biophys. J.* **1987**, *52*, 693−706. (b) Brochon. J.-C. *Methods Enzymol.* **1994**, *240*, 262−311.
(28) Lakowicz, J. R. *Principles of Fluorescence Spectroscopy*, 2nd ed.; Kluwer Academic/Plenum: New York, 1999.
(29) Klymchenko, A. S.; Pivovarenko, V. G.; Demchenko, A. P. *Spectrochim. Acta, A* **2003**, *59* (4), 787−792.
(30) Valeur, B. *Molecular Fluorescence*; Wiley-VCH: Weinheim, 2002; p 42.
(31) Laws, W. R.; Brand, L. *J. Phys. Chem.* **1979**, *83*, 795−802.
(32) Davenport, L.; Knutson, J. R.; Brand, L. *Biochemistry* **1986**, *25*, 1186−1195.
(33) According to the simplified solution of eqs 8, $|\alpha_1^{T^*}|$ is taken equal to $|\alpha_1^{N^*}|$.[6] This simplification affects only the absolute values of relative intensities of the obtained two band TRES spectra and does not affect the time dependent changes.
(34) Lakowicz, J. R. *Priciples of Fluorescence Spectroscopy*; Plenum Press: New York, 1983.
(35) The absolute values of k_+ cannot be calculated from the eq 7 using our data, because our measurements did not allow us to obtain the absolute values of $\alpha_1^{T^*}$ and $\alpha_2^{T^*}$.
(36) Swinney, T. C.; Kelley, D. F. *J. Chem. Phys.* **1991**, *95*, 10369−10373.
(37) Borgis, D. C.; Lee, S.; Hynes, J. T. *Chem. Phys. Lett.* **1989**, *162*, 19−26.
(38) Cukier, R. I.; Morillo, M. *J. Chem. Phys.* **1989**, *91*, 857−863.
(39) Sytnik, A.; Gormin, D.; Kasha, M. *Proc. Natl. Acad. Sci. U.S.A.* **1994**, *91*, 11968−11972.
(40) Reynolds, L.; Gardecki, J. A.; Frankland, S. J. V.; Horng, M. L.; Maroncelli. M. *J. Phys. Chem.* **1996**, *100*, 10337−10354.
(41) Demchenko, A. P. *Luminescence* **2002**, *17*, 19−42.
(42) (a) Demchenko, A. P. *Biochim. Biophys. Acta* **1994**, *1209*, 149−164. (b) Vincent, M.; Gallay, J.; Demchenko, A. P. *J. Phys. Chem.* **1995**, *99*, 14931−14941.
(43) Strickler, S. J.; Berg, R. A. *J. Chem. Phys.* **1962**, *37*, 814−822.
(44) Demchenko, A. P.; Klymchenko, A. S.; Pivovarenko, V. G.; Ercelen, S. In *Fluorescence Spectroscopy, Imaging and Probes—New Tools in Chemical, Physical and Life Sciences*; Kraayenhof, R., Visser, A. J. W. G., Gerritsen, H. C., Eds.; Springer Series on Fluorescence Methods and Applications; Springer-Verlag: Heidelberg, Germany, 2002; Vol. 2, pp 101−110.
(45) Demchenko, A. P.; Klymchenko, A. S.; Pivovarenko, V. G.; Ercelen, S.; Duportail, G.; Mely, Y. *J. Fluorescence* **2003**, *13*, 291−295.
(46) Klymchenko, A. S.; Pivovarenko, V. G.; Ozturk, T.; Demchenko, A. P. *New J. Chem.* **2003**, *27*, 1336−1343.